Materials Today Communications 52 (2026) 115228

Contents lists available at ScienceDirect

Materials Today Communications

journal homepage: www.elsevier.com/locate/mtcomm

Turning unsorted stranded seaweeds into biocomposites

Nicole Canzian [a], Gioele Foltran [a,b,*], Valentina Beghetto [a,c,d]

[a] Dipartimento di Scienze Molecolari e Nanosistemi, Università Ca' Foscari Venezia, Via Torino 155, Venezia 30172, Italy
[b] Dipartimento di Architettura e Disegno Industriale, Università della Campania "Luigi Vanvitelli", Via San Lorenzo-Abazia di San Lorenzo, 81031, Aversa (CE), Italy
[c] Crossing S.r.l., Viale della Repubblica 193/b, Treviso 31100, Italy
[d] Consorzio Interuniversitario per le Reattività Chimiche e La Catalisi (CIRCC), Via C. Ulpiani 27, Bari 70126, Italy

ARTICLE INFO

Keywords:
Biocomposite
Polybutylene succinate
PBS
Seaweeds
Epoxidized soybean oil

ABSTRACT

The valorisation of stranded seaweeds (SW) represents a promising strategy to transform an environmental burden into a renewable resource for sustainable materials. In this work, SW collected from coastal areas were tested as bio-fillers for the production of polybutylene succinate based biocomposites. Composites containing 10, 20, and 30 wt% SW were prepared by melt mixing and injection moulding. The effect of epoxidized soybean oil (EP, 2–6 wt%) as a bio-based compatibilizer/plasticizer was also evaluated. Thermal (DSC, TGA), mechanical (tensile strength, elongation at break, Young's modulus), morphological (SEM), surface (contact angle), colorimetric, and ATR-FTIR analyses were performed. Results showed that SW acts as a nucleating agent, increasing the crystallization temperature and slightly enhancing the crystallinity degree of polybutylene succinate, while maintaining a melting temperature comparable to the neat polymer (~114 °C). Although tensile strength decreased with increasing filler content, the addition of 6 wt% EP significantly improved elongation at break and interfacial adhesion, as confirmed by SEM and ATR-FTIR analyses. Thermal stability remained suitable for conventional processing. Soil burial tests showed enhanced biofragmentation of SW-containing composites, with the highest weight loss (~58% after 183 days) observed for P-SW20-EP6 and P-SW30-EP6. Overall, P-SW20-EP6 emerged as the best compromise between mechanical performance, thermal stability, and sustainability. This study demonstrates the feasibility of directly employing unsorted stranded seaweeds as fillers in PBS biocomposites, offering a scalable and environmentally sound valorisation route.

1. Introduction

Global plastic production reached approximately 413.8 million tons in 2023, only 1% of which was derived from biobased sources [1]. Despite their currently limited market share, biobased plastics present several notable advantages compared with their fossil-based counterparts, including lower reliance on non-renewable resources and improved biocompatibility [2–4]. Life cycle assessment studies further indicate that, depending on the type of feedstock, product design, and intended application, biobased plastics can achieve substantial reductions in CO_2 emissions relative to conventional petrochemical plastics [5–8]. Therefore, these materials are considered strategic in supporting the EU to lower greenhouse gas emissions and reach its net-zero objectives [9–11].

Within the broader framework of the European Green Deal and the United Nations 2030 Agenda [12], there is growing interest on the development of sustainable and biodegradable materials capable of aligning economic development with environmental protection goals [13–18].

However, the increase in biopolymer production also raises several critical concerns. These include limitations in feedstock availability, potential competition with food and feed supply chains [19,20], land-use pressure, and risks for biodiversity associated with the cultivation of non-native crops dedicated to biorefinery systems [21–23].

A promising strategy to enhance the sustainability of bioplastics involves the use of by-products and waste from the agri-food industry as alternative feedstocks [24–26]. In particular, organic food waste, typically rich in lignocellulosic fractions, can serve as a bio-based filler in the production of biocomposites. These materials are generally obtained by incorporating varying weight percentages of waste-derived fillers into a virgin biopolymer matrix, followed by conventional processing techniques such as extrusion and injection molding [15,27,28].

Through this approach, biocomposites can contribute to lowering the demand for virgin biopolymers, reducing manufacturing costs,

* Corresponding author at: Dipartimento di Scienze Molecolari e Nanosistemi, Università Ca' Foscari Venezia, Via Torino 155, Venezia 30172, Italy.
E-mail address: gioele.foltran@unicampania.it (G. Foltran).

https://doi.org/10.1016/j.mtcomm.2026.115228
Received 10 March 2026; Received in revised form 15 April 2026; Accepted 20 April 2026
Available online 21 April 2026
2352-4928/© 2026 The Author(s). Published by Elsevier Ltd. This is an open access article under the CC BY license (http://creativecommons.org/licenses/by/4.0/).

enhancing market competitiveness, and improving the management and valorization of agri-food waste [29–31]. Among thermoplastic polymers, polylactic acid, polybutylene succinate, and polybutylene adipate terephthalate are particularly attractive for biocomposite production, because of their commercial availability, renewable origin, and good processability [2,16,32].

Polybutylene succinate, in particular, is an aliphatic biodegradable polyester with thermal, mechanical, and physical properties comparable to those of polypropylene [2,33]. Owing to these characteristics, it has been extensively investigated as a matrix for biocomposites reinforced with various lignocellulosic fillers, including jute fibers [13,34–36], beer spent grain [37–39], grape pomace [40,41], almond shell flour [42,43], coffee grounds [44–46], potato peels [47], and wheat bran [48,49].

In this context, it is noteworthy that seaweeds, despite being an abundant renewable resource, has only marginally been explored as an alternative to agri-food residues, for the production of biocomposites. Several algae species, including *Gelidiella acerosa*, *Gracilaria*, and *Gelidium amansi*, are extensively cultivated and processed worldwide for applications in cosmetics, pharmaceuticals, food products, pigments, fertilizers, and biofuels [50–54]. Although global algal variety is estimated to exceed 164,000 species, only about 9800 of these are classified as seaweeds and merely 0.17% of them are harvested for commercial applications [55,56], while naturally proliferating seaweeds in marine and freshwater environments remain largely underutilized [57].

At the same time, eutrophication has intensified the uncontrolled growth of seaweeds, disrupting aquatic ecosystems and altering water quality. Massive seaweed blooms pose serious challenges to lagoon and coastal environments, negatively affecting shellfish populations and other aquatic organisms. Moreover, the removal of seaweeds often generates additional environmental burdens, as large amounts of rapidly degradable organic matter accumulate along riverbanks and shorelines. This situation leads to significant ecological and socioeconomic consequences, particularly for the fishing and aquaculture sectors. For instance, in the Po Delta (Italy), seaweed overgrowth (up to 10 kg/m^2) contributed to a decline of more than 30% in clam and mussel production in 2022.

Very few works have been reported in the literature regarding the use of algae waste, recovered after agarose or oil extraction, as bio filler for fossil-based [58–63], or bio-based [64–72] composites production by extrusion and injection moulding. Additionally, protocols for the production of biodegradable biocomposites often require pretreatments of the algae by bleaching or washing in soda or the use of toxic compatibilizing agents generating environmental concern [64–70].

An interesting study by Rosdi reported a straightforward protocol for producing PLA-based biocomposites using a selected red algal species (*Kappaphycus alvarezii*) that was simply milled and sieved prior to processing [71]. Furthermore, Bulota and co-workers demonstrated that PLA biocomposites prepared with three different types of algae (red, brown, or green), exhibited comparable physical-mechanical properties, suggest that seaweeds, even when not specifically selected or pretreated, could serve as effective fillers in biocomposite production [73,74]. This approach is particularly attractive, as it may enable sustainable strategies for the valorization and recycling of large quantities of unselected and untreated seaweed biomass.

This work is the first of its kind validation study of the use of unsorted stranded seaweeds (SW) as bio-fillers to produce polybutylene succinate (P) biocomposites. SW were only milled and sieved after washing and drying. The influence of the wt% of bio filler (between 10 and 30 wt%) and of epoxidized soybean oil used as additive (EP, between 2 and 6 wt %) on the physical-mechanical (tensile strength, elongation at break, Young's modulus, contact angle, colour), thermal characteristics (DSC, TGA) and ATR-FTIR, SEM of the biocomposites were studied and compared to virgin P. Biodegradability in soil was also assessed. The hypothesis is that considering the relatively high amount of carbohydrates present in SW it can be successfully employed as filler for the production of P-SW biocomposites. Additionally, the epoxide moiety of EP may interact with the hydroxyl groups of the lignocellulosic fraction of SW, while the apolar tail with the P chains through hydrophobic interactions, leading to an improved compatibility between the matrix and the filler, improving the properties of the biocomposite.

2. Material and methods

2.1. Materials

Polybutylene succinate (melt flow rate 26 g/10 min, melting temperature 114 °C) was purchased from Tunhe, epoxidized soybean oil (Esopol, EP) was supplied by Chimitrade (Italy) and used as received. Seaweeds (SW) were collected from the "Sacca di Goro" Ferrara (Italy).

2.2. Methods

2.2.1. Seaweed composition

Quantification of ash was determined according to the literature [75]. Dried ground seaweed (0.6962 g) was placed in a 25 mL flask with 5 mL of 72% w/w H_2SO_4 and heated under reflux for 4.5 h. The mixture was filtered on a weighed Gooch, washed with water, and oven dried at 104 °C for 24 h. The black solid obtained, was transferred into a weighed crucible and placed in a muffle furnace for 5 h at 600 °C and ash content determined.

Quantification of lignin was determined according to the literature [75]. Dried ground seaweed (0.7160 g) was placed in a flask with 5 mL of 72% w/w H_2SO_4 and stirred at room temperature for 1 h. Then, 150 mL of water were added, heated under reflux for 3 h, filtered on a weighed Gooch and washed with water to neutral pH. The residue was oven dried at 80 °C for 72 h, yielding 0.0637 g of a black solid. The lignin content was determined by subtracting the ash content from this value.

Seaweed crude protein content was determined by quantifying the total nitrogen content on dry material. After placing the material in the oven (70 °C, overnight), it was hydrolysed in an acid medium (pH 2.0) at 320 °C and 30 bar, using a Speedwave Xpert – Berghof (Germany) to transform all the nitrogen to ammonia ions. Then, ammonia ions were converted to ammoniacal nitrogen at alkaline pH, recovered by distillation, conveyed in a boric acid solution and analysed with colorimetric Nessler's method [76]. Then, the nitrogen concentration was multiplied by the conversion factor of 6.25 according to IRSA-CNR, 2003 [77]. Further SW carbohydrate content was determined according to the procedure described by Pangestuti [78]. Total carbohydrate content was estimated using Eq. 1:

$$carbohydrate\% = 100 - ash\% - lignin\% - protein\% - moisture\% \quad (1)$$

2.2.2. Preparation of seaweed filler

Seaweeds were washed with water to remove sand and dirt. Wet seaweeds were air dried for 3 days, grinded using a ball mill PM100 (Retsch, DE). The grinding process was performed using a ball mill with the following specifications: 80 mL zirconia jar, 5 zirconia balls (diameter 20 mm), 350 rpm, 1 h. To prevent overheating and potential thermal degradation of the seaweed biomass, the process was set with intervals of 10 min of active milling followed by 3 min pause. The fine powder was sieved to < 90 μm size then dried at 50 °C to a constant weight before use. The particle size distribution of the SW, determined with Laser Mastersizer 3000 (Malvern Panalytical), is reported in Figure S1. Additionally optical microscopy analysis of < 90 μm meshed SW was performed with a Digital Microscope "4 K Keyence VHX-X1" (Keyence Corporation, Osaka, Japan) (see Figure S2).

2.2.3. Biocomposites preparation

The biocomposite materials were prepared in two steps. First, PBS was mixed with different percentages of seaweed powder and additive (see Table 1) in a melt mixer (Plastograph EC, Brabender, Duisburg DE) at 140 °C for 30 min at 80 rpm. The materials were removed from the

Table 1
Composition of biocomposites mixtures and identification codes of the samples.

Sample name	P (%wt)	SW (%wt)	EP (%wt)
P	100	-	-
P-SW10	90	10	-
P-SW10-EP2	90	10	2
P-SW10-EP4	90	10	4
P-SW10-EP6	90	10	6
P-SW20	80	20	-
P-SW20-EP2	80	20	2
P-SW20-EP4	80	20	4
P-SW20-EP6	80	20	6
P-SW30	70	30	-
P-SW30-EP2	70	30	2
P-SW30-EP4	70	30	4
P-SW30-EP6	70	30	6

mixer and grinded into small pieces with a coffee grinder to obtain pellets. The pellets were used in the injection moulding (HAAKE MiniJet II (Thermo Fisher Scientific, USA), 900 bar, cylinder temperature 150 °C, moulder temperature 30 °C) to produce dumbbell-specimen.

2.2.4. Differential scanning calorimetry (DSC)

A small piece of biocomposite was weight (about 10 mg) in the crucible and analyses were carried out with a DSC 3 (Mettler Toledo, USA) under nitrogen atmosphere (40 mL/min); an empty crucible was used as reference. The samples were rapidly heated to 160 °C and maintained for 5 min, followed by cooling to 20 °C with a rate of 10 °C/min, then heated again to 160 °C with a rate of 10 °C/min [79]. DSC thermograms show two different curves, during the cooling there is an exothermic peak related to the crystallization process of the polymer, the heating instead shows the endothermic melting peaks. From this curve crystallization temperature (T_c), melting temperature (T_{m1}/T_{m2}) were identified and crystallization enthalpy (ΔH_c) can be determined by integrating the area under the crystallization peak, by Eq. 2:

$$\chi_c(\%) = \frac{\Delta H_c}{\Delta H_m^0 \bullet (1 - W_f)} \bullet 100 \quad (2)$$

where ΔH_m^0 is the enthalpy of 100% crystalline PBS (110.3 J/g), and W_f is the weight fraction of the filler (seaweed) in the composites, which is totally amorphous.

2.2.5. Thermogravimetric analysis (TGA)

A piece of biocomposite (about 8 mg) was put in the crucible, and the measure were carried out thanks to a STAR PT-1000 (Perkin Elmer), under a nitrogen flux (20 mL/min), the sample was heated from 30 °C to 600 °C with a rate of 10 °C/min. Derivative thermogravimetric (DTG) curves were also calculated.

2.2.6. Mechanical testing

Tensile tests have been performed on dumbbell-specimen (Type IV) in accordance with ASTM D638 and ASTM D618 standards [80,81], all specimens were conditioned for at least 40 h at room temperature inside a desiccator containing saturated $MgCl_2$ solution (33% final humidity). The tests were then performed immediately after removing the samples from the controlled environment. Tensile parameters were determined using Lonos Test machine dynamometer (Brescia, IT) equipped with a 50 kN load cell. Tests have been conducted at room temperature with a 10 mm/min clamp separation speed. The reported data of Young's modulus (E), tensile strength (σ_r) and elongation at break (ε_r) are the average values of at least three determinations.

2.2.7. ATR-FTIR

The Fourier transform infrared (ATR-FTIR) spectra were acquired from a thin slice of biocomposite with a Perkin Elmer spectrum with $LiTaO_3$ detector. Measurements were recorded from 400 to 4000 cm^{-1}, using 100 scans at a resolution of 1 cm^{-1}.

2.2.8. Water contact angle

Contact angle measurements were performed using a Celeston Digital Microscope (USA). A drop of 10 μL of water was placed on the surface of the dumbbell-specimen and contact angle value was recorded after drop stabilization (10 s). Picture was processed using ImageJ software for contact angle measurement.

2.2.9. Scanning electron microscopy (SEM)

Prior to the observations the tensile-fractured surface of the samples were sputter-coated with a thin layer of gold (40 mA for 15 s). The sample was observed under a field-emission scanning electron microscope (Hitachi High-Tech TM3000, Tokyo) with high sensitivity four-sector semiconductor BSE detector. The micrographs were acquired at 500x and 40x magnification.

2.2.10. Colour analysis

The surface colour of the samples was characterized via a CM 2600d Spectro-colorimeter (Konica Minolta Sensing Inc. Osaka, Japan), operating in SCE mode with a D65 light source. For each biocomposite, triplicate readings were taken across random surface areas to obtain representative L* (lightness), a* (redness) and b* (yellowness) coordinates. Furthermore, darkening induced by the high-temperature molding stages was quantified through the Browning Index (BI), calculated using Eq. 3:

$$BI = [(100 \bullet (x - 0.31))/0.17] \quad (3)$$

Where x is obtained from Eq. 4:

$$x = [(a^* + 1.75 \bullet l^*)/(5.645 \bullet l^* + a^* - 0.3012 \bullet b^*)] \quad (4)$$

2.2.11. Biofragmentation

The electrical conductivity 0.8 dS/m, pH (pH 8.17 ± 0.27), dry bulk density (220 kg/m^3) and C/N ratio (C (%) 33.70 ± 1.66, and N (%) 1.51 ± 0.09) of the universal soil were measured according to EN 13038, EN 13037, EN 13041 [82–84]. The soil was poured into an aluminium tray. Samples with different percentage of SW and EP 6 wt% were weight and buried in the soil to a depth of approximately 10 mm. The trays were kept at ambient temperature and sprayed with water twice a day to maintain the moisture. At different times (every week for the first month and then every month), samples were carefully taken out and dried. After that they were weighed and photographed for visual analysis (Figure S3), according to Jaramillo [85,86].

2.2.12. Statistical analysis

All tensile data were generated at least in triplicate and statistical significance was assessed via one-way analysis of variance (ANOVA) followed by Tukey's Honestly Significant Difference (HSD) post-hoc test for multiple comparisons. The test was specifically conducted to compare different groups containing the same seaweed percentage. A p-value < 0.05 was considered statistically significant. All analyses were performed using OriginLab software (OriginLab Corp., Northampton, MA, USA).

3. Results and discussion

3.1. Chemical analyses of seaweeds

The chemical composition of stranded seaweeds is reported in Table 2 and was measured as reported in the methods Section 2.2.1. Since the composition of seaweeds can change according to the species, geographical area, climate conditions, among others, only seaweeds collected in one campaign were used in this work, to avoid excessive variabilities [87].

Table 2
Composition of stranded seaweeds.

Composition of seaweeds	%
Carbohydrates	52.6
Lignin	7.2
Protein	27.0
Ash	1.7
Moisture	11.5

It is nevertheless important to consider that according to the literature PLA biocomposites prepared with red, brown, or green algae, have been reported to exhibit comparable physical-mechanical properties, suggesting that the composition variability of SW is not significant enough to play a crucial role in influencing biocomposites properties [73,74].

3.2. Thermal properties of bio composites

Thermal properties of all specimens were measured by DSC (see Table 3) giving information about melting temperature (T_{m1}/T_{m2}), crystallization temperature (T_c) and enthalpy (ΔH_c) and crystallinity degree (χ_c). P and biocomposite samples were heated twice to suppress thermal history and DSC data reported are those collected during cooling and second heating run [30,88].

The DSC thermograms of P-SW10, P-SW20 and P-SW30 (see Figure S4-S6) show a characteristic double melting peak T_{m1} and T_{m2} between 100 °C and 140 °C, a phenomenon typical of polyesters like PBS, which is generally explained by the melting-recrystallization-remelting model [88–90]. The lower melting temperature (T_{m1}) corresponds to the melting of the less-perfect lamellae formed during the first cooling of the melt. The increase of T_{m1} from 101.8 °C to 103.9 °C for P-SW20-EP6 and P-SW30-EP6 suggests that SW promotes the formation of thicker or more ordered primary lamellae. These crystals possess higher thermodynamic stability, thus requiring more energy (higher temperature) to melt. Consistent with literature data, the higher melting temperature (T_{m2}) of all samples remained nearly unchanged (approximately 114 °C, Table 3) and comparable to that of neat P (Figure S7) [39,91], indicating that SW does not alter the overall crystal structure or the melting point of P.

Table 3
Thermal properties of all samples tested measured by DSC and TGA analysis.

	DSC					TGA	
Sample name	T_c (°C)	ΔH_c (J/g)	χ_c (%)	T_{m1} (°C)	T_{m2} (°C)	$T_{10\%WL}$[(a)] (°C)	T_{peak} (°C)
P	74.2 ± 1.2	65.4 ± 2.3	59.3 ± 2.1	90.0 ± 0.2	113.9 ± 0.3	357.8	412.8
P-SW10	84.1 ± 0.4	61.7 ± 0.5	62.2 ± 0.5	101.6 ± 0.3	115.1 ± 0.1	364.8	407.0
P-SW10-EP2	83.6 ± 0.2	60.0 ± 0.9	60.5 ± 0.9	100.7 ± 0.2	114.8 ± 0.3	358.8	407.5
P-SW10-EP4	83.6 ± 0.1	59.9 ± 0.8	60.3 ± 0.8	101.4 ± 0.1	114.4 ± 0.2	356.5	405.0
P-SW10-EP6	83.5 ± 0.1	60.7 ± 0.6	61.2 ± 0.6	101.0 ± 0.2	114.4 ± 0.1	359.5	406.3
P-SW20	85.3 ± 0.3	55.9 ± 0.1	63.4 ± 0.2	102.5 ± 0.2	114.6 ± 0.3	330.5	407.0
P-SW20-EP2	86.0 ± 0.2	54.0 ± 0.1	61.2 ± 0.2	103.4 ± 0.1	115.1 ± 0.1	338.5	404.5
P-SW20-EP4	85.8 ± 0.2	52.9 ± 0.4	59.9 ± 0.5	103.0 ± 0.2	114.8 ± 0.1	336.0	404.8
P-SW20-EP6	85.2 ± 0.1	52.4 ± 0.7	59.4 ± 0.7	101.8 ± 0.3	114.4 ± 0.2	330.0	404.5
P-SW30	86.7 ± 0.4	47.3 ± 0.9	61.3 ± 0.6	103.5 ± 0.2	114.5 ± 0.2	278.5	401.3
P-SW30-EP2	87.7 ± 0.1	48.2 ± 0.2	62.5 ± 0.2	103.7 ± 0.1	114.4 ± 0.3	308.8	402.4
P-SW30-EP4	87.7 ± 0.1	46.5 ± 0.4	60.2 ± 0.5	103.8 ± 0.1	114.4 ± 0.1	308.8	402.4
P-SW30-EP6	87.7 ± 0.3	47.0 ± 0.4	60.8 ± 0.5	103.9 ± 0.2	114.2 ± 0.2	300.8	401.9

(a) WL – weight loss

The cooling thermograms reveal that the incorporation of SW significantly affects the crystallization kinetics of P. The shift of the crystallization temperature (T_c) toward higher values as the SW content increases (from 62.7 °C up to 84.1 °C, Table 3) is a clear indication of a heterogeneous nucleation effect [79]. The SW particles act as pre-existing nuclei in the polymer melt, reducing the free energy barrier required for the formation of the first crystalline structure, as reported for PBSA/ATP systems [92]. Since Turco [89] reported that T_c of polybutylene succinate blends containing 2.5 wt% EP (P-EP2.5) is the same as that of the pristine polymer, the increase observed in T_c, is to be attributed exclusively to SW. Thus, as for P-EP also for P-SW composites, EP mainly acts as a plasticizer, allowing higher chain mobility and favouring polymer crystallization. This evidence suggests that EP does not substantially influence the structural reorganization of the polymer chains during cooling but is able to promote crystallization by chain rearrangement, which influences physical mechanical properties as discussed below. This is further supported by an increase in χ_c from 59.3% for P to values between 60.3% and 63.4% for P-SW specimens (Table 3).

TGA curves of all specimens tested are reported in Fig. 1 and Figure S8, S9. The thermal degradation of SW (grey line in Fig. 1a) shows a multi-step degradation pathway. The first weight loss between 50 °C and 150 °C, is attributed to residual humidity in the sample together with volatiles. The second degradation, between 160 °C and 300 °C is related to carbohydrate decomposition, whereas protein degradation occurs between 320 °C and 450 °C [93]. It is interesting to note that TGA profiles of P-SW10, P-SW20, P-SW30, show a weight loss between 250 °C and 360 °C which is close to the wt% of filler present (10–30 wt%, see Table in Fig. 1a) and is a consequence of SW degradation. Weight loss between 350 °C and 450 °C is due to total decomposition of P and proteins in SW, while above 450 °C the degradation curves of P-SW10, P-SW20, P-SW30 follow the same trend of that of pure SW.

Data from DTG show a modest decrease in T_{peak} for composites containing the bio filler, which may be attributed to the higher mobility of the polymeric chains as a consequence of reduced adhesion interactions between SW and P (Table 3, Fig. 1b) [88].

In Table 3 are also reported the temperatures at which 10 wt% of the sample is loss ($T_{10\%WL}$). An improvement of 7 °C was measured for P-SW10 compared to P, and moderately also for P-SW10 containing between 2 and 6 wt% EP. More significant influence on $T_{10\%WL}$ was evidenced between P-SW20 and P-SW30 with and without EP, with an increase in $T_{10\%WL}$ of over 30 °C, evidenced by a strong thermal improvement of the biocomposites due to the presence of EP (Table 3). In any case the degradation temperature of all biocomposites tested is highly above processing temperatures ($\leq$ 150 °C), allowing for a safe and standardizable industrial process.

3.3. Mechanical properties of bio composites

Unsorted stranded seaweeds were grinded and meshed below 90 μm. This specific mesh was chosen in order to achieve a high filler distribution within the biocomposite. In fact, preliminary studies, showed that higher granulometry ($<$ 250 μm), gave a non-homogeneous filler dispersion, leading to visible clusters and potential mechanical weak points within the biocomposite (Fig. 2a) [94]. Reducing the particle size increases the specific surface area, which typically enhances the interfacial adhesion between the seaweed filler and the polymer matrix, and improves the bio filler dispersion within P (Fig. 2b), thus seaweeds were meshed down to $<$ 90 μm (see Figure S1) and optical images (Figure S2) evidences their irregular flake like shape.

Dumbbell specimens of P, and all biocomposites were prepared and

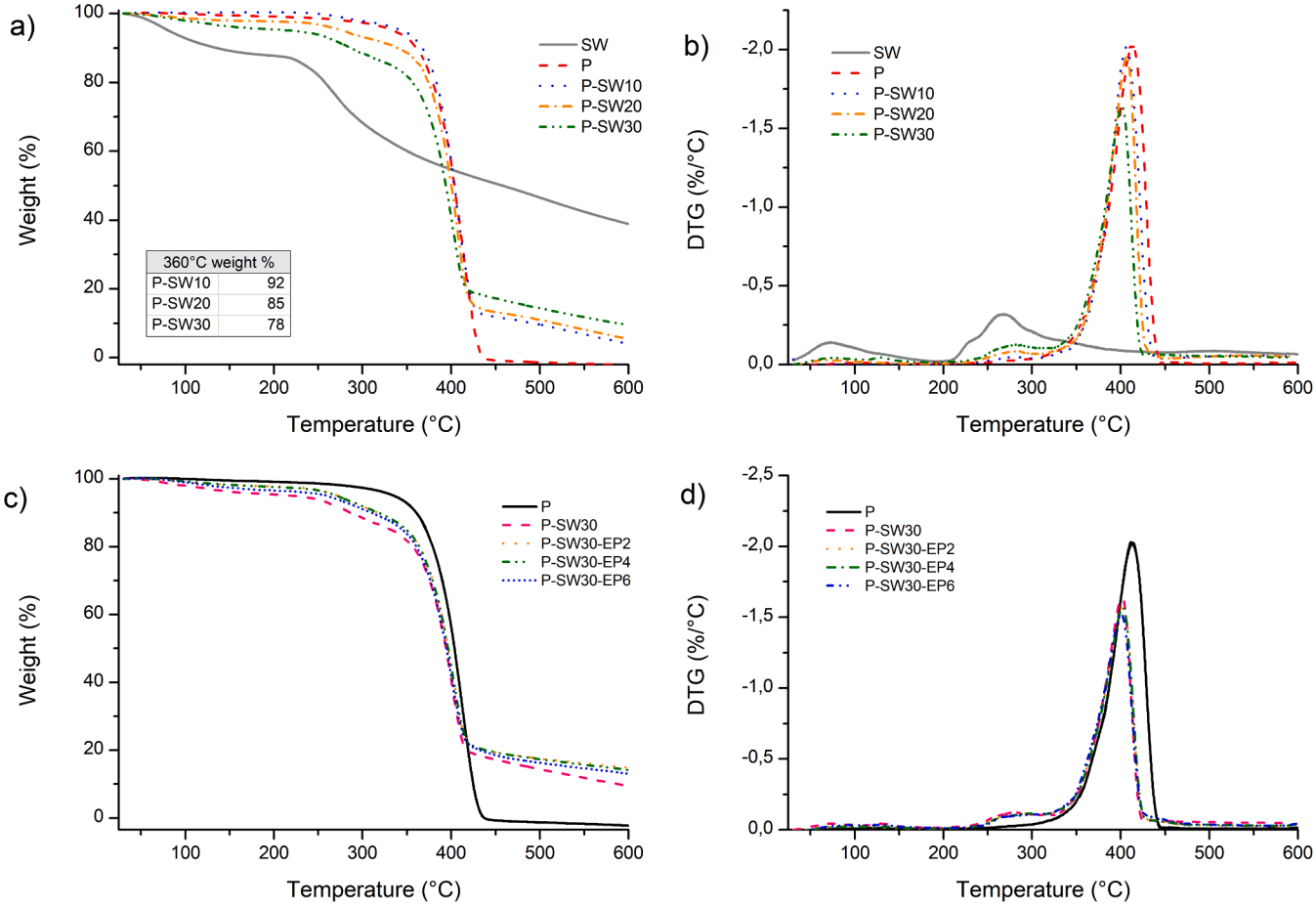

Fig. 1. a) TGA of SW, P, P-SW. b) DTG of SW, P, P-SW. c) TGA of P, P-SW30, P-SW30-EP. d) DTG of P, P-SW30, P-SW30-EP.

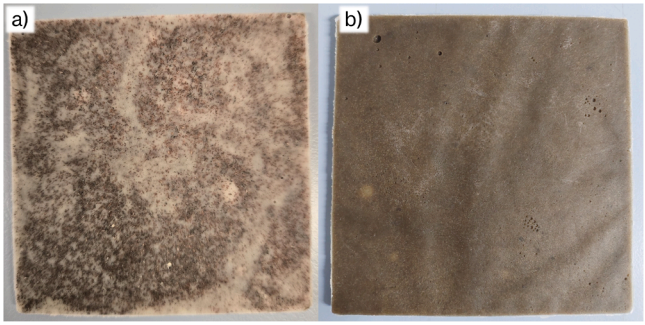

Fig. 2. Samples of P-SW10 with a) seaweeds mesh < 250 μm and b) seaweeds mesh < 90 μm.

used to measure tensile strength (σ_r, MPa), elongation at break (ε_r, %) and Young's modulus (E, MPa) as reported in Fig. 3. Different P-SW samples containing variable wt% of EP (identified with different colours) are grouped according to wt% of SW present to better highlight changes in the physical mechanical properties of specimens tested.

According to data reported in Fig. 3a, tensile strength of the biocomposites gradually decreases compared to P as the wt% of SW increases, in accordance with the literature [95,96]. Nevertheless, it is interesting to note that σ_r of P-SW20 (13.17 MPa) is comparable to those of P/sodium alginate 80/20 wt/wt (22.50 MPa) or P/beer spent grain 70/30 wt/wt biocomposites (16 MPa), which have been demonstrated to possess good thermoplastic characteristics and ease of processability [39,88].

The addition of EP unfortunately further decreased σ_r as reported by Turco for P-EP composites [89]; notably, this downward trend in σ_r was observed across all investigated SW weight fractions when 6 wt% of EP was added ($p < 0.05$). Conversely, it is worth noting that 6 wt% of EP consistently improves the ε_r ($p < 0.05$). In terms of mechanical performance, the elongation at break effectively doubles across all SW wt% compared to the corresponding biocomposites without EP (Fig. 3b).

Regarding Young's modulus, no significant variations were observed, with values remaining comparable to P for all samples; however, a significant decrease ($p < 0.05$) is clearly detected in cases where 6 wt% EP was added (Fig. 3c). In general, these data are among the best values reported in the literature for P biocomposites, since generally ε_r does not exceed 3–6% and very stiff materials with high E are obtained [91,97]. To best of our knowledge most similar results were obtained by Liminana for the preparation of P/almond composites 70/30 containing 4.5 wt% of EP ($\varepsilon_r = 13.1\%$) [98]. As reported in the literature, epoxidized vegetable oils may function as compatibilizing and plasticizing agents forming hydrogen bonds with both P and the bio filler, according to the mechanism reported in Fig. 4 [98]. Additionally, higher mobility of P chains may be generated due to the presence of the long hydrophobic chains of EP.

The nucleation effect observed via DSC induces a microstructural transition toward a more crystalline framework, which typically renders the matrix more brittle. However, the addition of EP enhancing polymer chains mobility, improves elongation at break. This suggests that while SW promotes a rigid crystalline structure, EP acts as an effective plasticizer, restoring the biocomposite ability to plastically deform and improving its overall energy dissipation capacity. Based on data reported above and to fully exploit waste materials as valuable resources

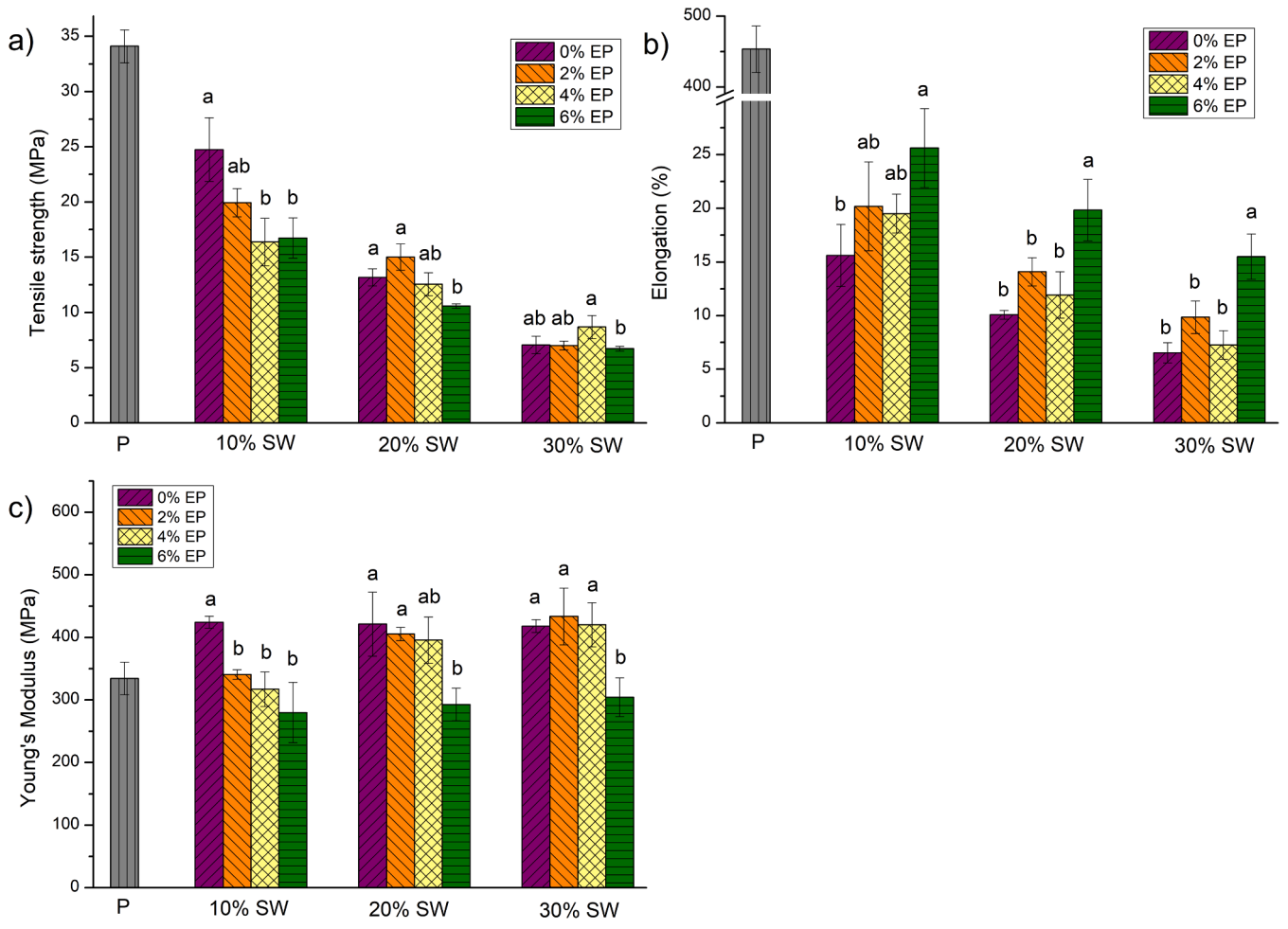

Fig. 3. Mechanical properties of P and biocomposite. a) Tensile strength (σ_r); b) Elongation at break (ε_r) c) Young's Modulus (E) (in the figures, different letters indicate significant differences $p < 0.05$ between groups).

within a circular economy framework, particularly for industrial applications, it is advantageous to incorporate the highest feasible amount of bio-filler into bio-composites. At the same time, achieving an effective balance is essential, since increasing bio-filler content can affect processability and may compromise the final mechanical and physical performance of the material. Physical-mechanical and thermal analysis reported indicate that P-SW20-EP6 can be considered the optimal formulation and therefore only specimens containing 6 wt% of EP were further characterized.

3.4. ATR-FTIR, water contact angle and SEM analysis

All biocomposites were characterized by ATR-Fourier Transform Infrared Spectroscopy analysis (ATR-FTIR, see Fig. 5 and Figure S10-S12). The vibrational frequency of the characteristic carbonyl group stretching (1714 cm^{-1}) in P are sensitive to weak interactions, such as hydrogen bonds and consequently, changes in this frequency, evidenced by ATR-FTIR, can give information on the compatibility between the polymer matrix and the filler [95,99]. In fact, spectra of P-SW10, P-SW20 and P-SW30 (Fig. 5a, b) show very similar profiles, apart from an increase in the wavenumber of the stretching vibration from 1714.25 to 1715.25 cm^{-1} between P and P-SW10, which indicates a decrease in compatibility. For SW loadings above 20 wt% the stretching vibration returns to the same values as for P. In contrast, when EP is added the wavenumber decreases compared to P (see for example Fig. 5c, d), which is consistent with the formation of interactions between the matrix and the filler, indicating a weakening of the carbonyl bond and lowering of the energy required for vibrational excitation [100].

Water contact angle data of P-SW10, P-SW20 and P-SW30 with 6 wt % of EP and without EP are reported in Fig. 6. P exhibits a moderate hydrophobic character with a contact angle of ~60°, and interestingly the incorporation of 20–30 wt% of SW did not substantially alter this value.

The presence of EP contributes to increase surface hydrophobicity compared to the same specimens prepared without EP and the hydrophobicity of P-SW30-EP6 is 10% higher than that of the starting polymer P, in agreement with the literature [101].

Scanning electron microscopy (SEM) micrographs at 500x magnification of P-SW20 and P-SW20-EP6 dumbbell fractured surface, after tensile test, are shown in Fig. 7. The fracture surface of P-SW20 appears irregular and highly non-uniform. This surface morphology clearly indicates insufficient interfacial bonding between the polymer matrix and the filler. Numerous cavities and pronounced gaps can be observed around the filler particles, many of which seem to have detached from the matrix during fracture. These features evidence weak interfacial interactions and inadequate wetting of the hydrophilic SW filler by the hydrophobic PBS matrix, resulting in a predominantly brittle fracture behaviour.

The addition of 6 wt% of EP leads to a noticeable change in the fracture surface morphology, and the SW particles show a better degree of embedment within the polymer matrix, so that the fracture surfaces of P-SW20-EP6 are considerably denser and more uniform. Signs of particle pull-out are scarce, and the filler particles are more uniformly enveloped by the P matrix. These observations indicate that the EP

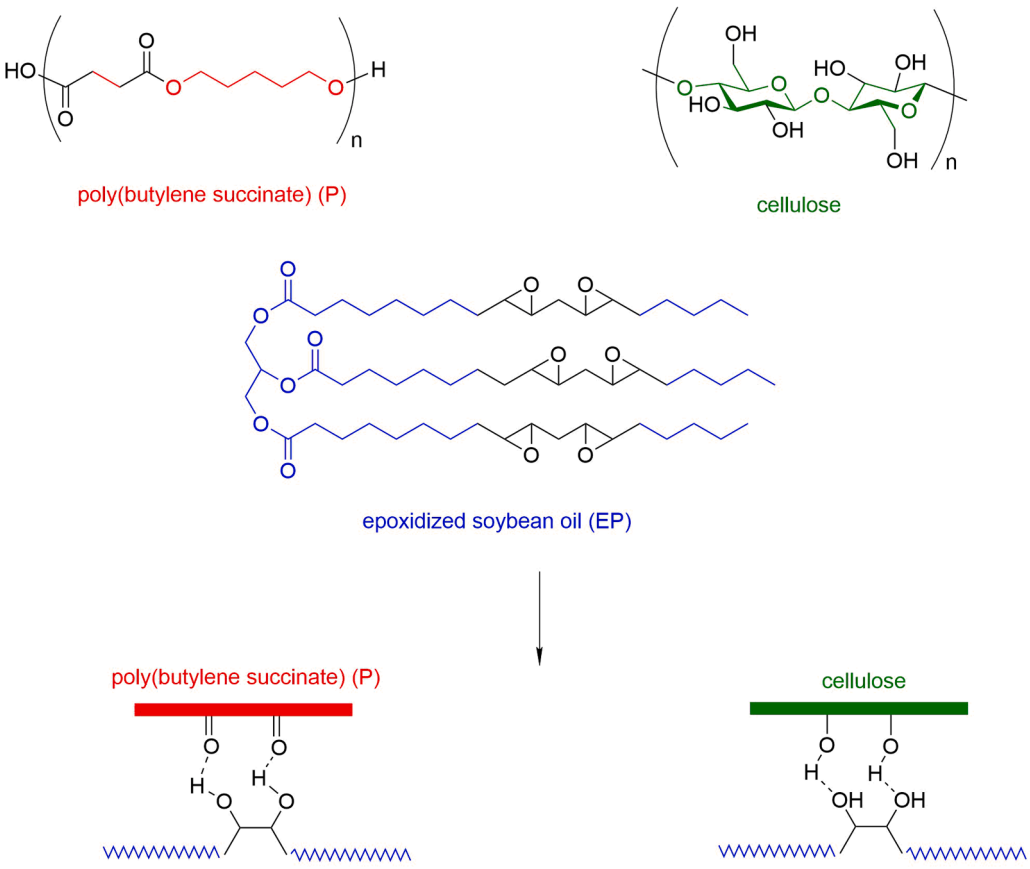

Fig. 4. Schematic representation of possible interactions within P and SW in the presence of EP.

additive enhances interfacial bonding between P and SW, enabling a more efficient and cohesive transfer of stress under mechanical loading. The progressive shift from a brittle, poorly bonded fracture surface in P-SW20 to a more compact and cohesive morphology at higher EP concentrations demonstrates that EP effectively strengthens interfacial adhesion, leading to improved overall compatibility between the composite components.

3.5. Colour analysis

Colorimetric parameters of all specimens (L*, a*, b*) and browning index (BI) (calculated as reported in the materials and method section) are summarized in Table 4. L* refers to the lightness coordinate ranging from 0 (black) to 100 (white), while a* (redness) and b* (yellowness). In general, color parameters are measured to assess information on the optical properties of biocomposites, which are particularly important for the final application, such as for example packaging, flowerpots among others [39,102].

As expected, the presence of the bio filler strongly reduces the brightness (L*) of the biocomposites compared to the pure polymer (P 80.49), with values ranging from L* 24.21 for P-SW10 to L* 20.63 for P-SW30, although increasing quantities of EP lead to a moderate improvement and leveraging of samples lightness (P-SW10-EP6 32.87 and P-SW30-EP6 27.85 respectively, Table 4), suggesting a partial mitigation of the darkening effect of SW [37,103]. Additionally in all cases, the presence of 6 wt% of EP generates maximum lightening with a significant increase in redness (a*) and yellowness (b*). In this case, the additive not only lightens but also intensifies the colour components that generate the brown hue.

3.6. Biofragmentation of biocomposites

The weight losses of the biocomposites after 6 months are reported in Fig. 8. The biocomposites exhibited a better biodegradation trend compared to the virgin polymer and, in all cases, the presence of EP improved biofragmentation and the highest weight loss (58%) was obtained for P-SW30-EP6 [104,105].

4. Conclusions

This study demonstrates for the first time, the feasibility of using unsorted, milled, and sieved stranded seaweeds as bio-fillers in polybutylene succinate biocomposites without chemical pretreatments. Seaweed incorporation (10–30 wt%) increased crystallization temperature and crystallinity of all samples, confirming a nucleating effect of SW, while maintaining melting temperatures similar to polybutylene succinate and compatible with industrial processing.

Although filler addition reduced tensile strength and ductility, the incorporation of 6 wt% epoxidized soybean oil improved interfacial adhesion, elongation at break, and surface hydrophobicity, as evidenced by SEM, ATR-FTIR, and contact angle analyses. Thermal stability remained adequate for melt processing.

Biodegradation tests highlighted a clear enhancement in soil biofragmentation with increasing seaweed content, further promoted by EP addition. Among the formulations investigated, P-SW20-EP6 provided the best balance between mechanical performance, thermal behavior, and biodegradability. Future studies will be devoted to analysing the influence on biocomposites physical-mechanical characteristics as a function of seaweeds variability and include a larger number of replicates to further improve statistical significance.

The direct use of naturally stranded, unsorted seaweeds represents a sustainable and scalable approach to valorise excess biomass, while

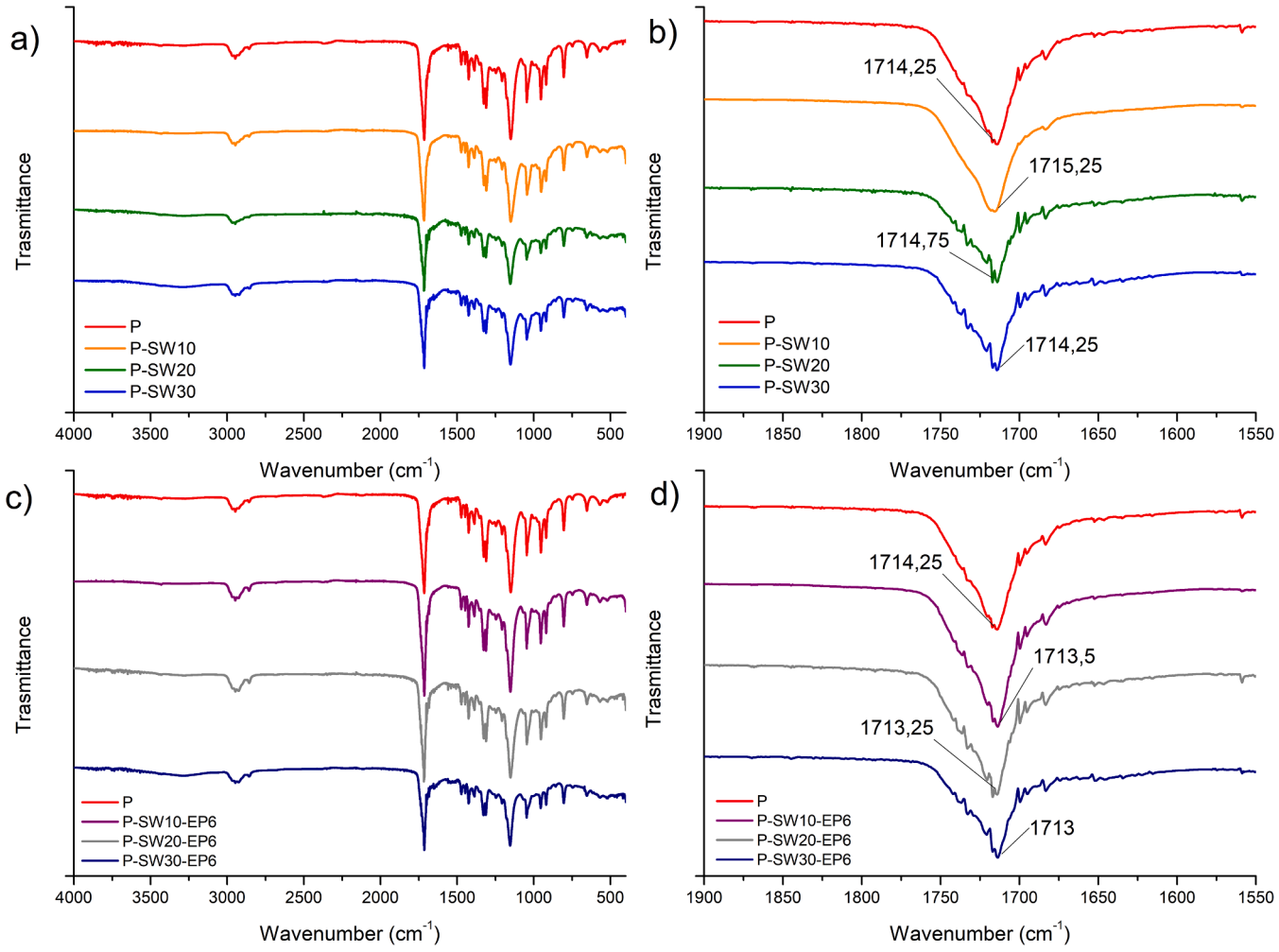

Fig. 5. ATR-FTIR spectra of a) P, P-SW. b) magnification between 1550 and 1900 cm-1. c) P, P-SW-EP6. d) magnification between 1550 and 1900 cm-1.

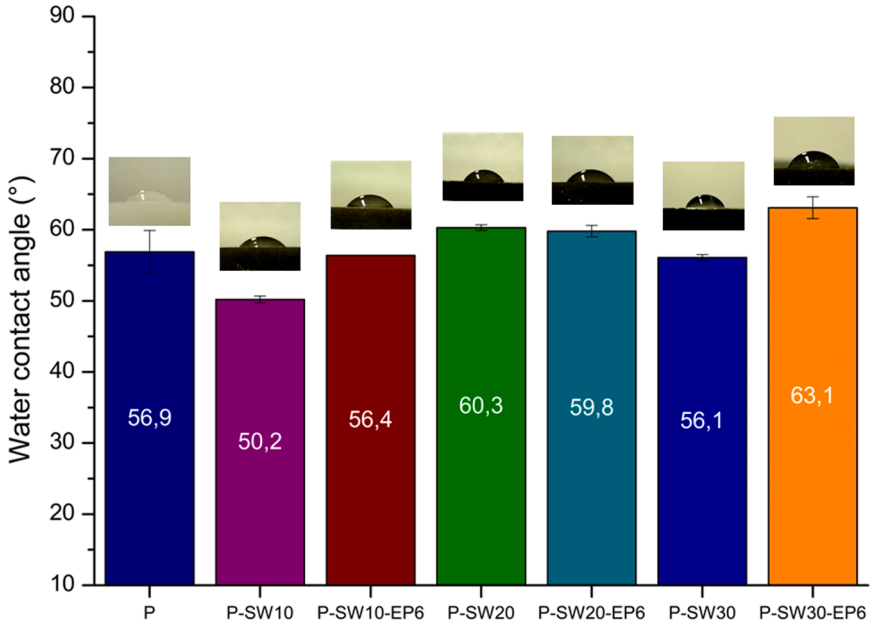

Fig. 6. Water contact angle of P and of P-SW10, P-SW20 and P-SW30 and corresponding composites containing 6 wt% of EP.

contributing to the development of environmentally friendly biocomposites within a circular economy framework.

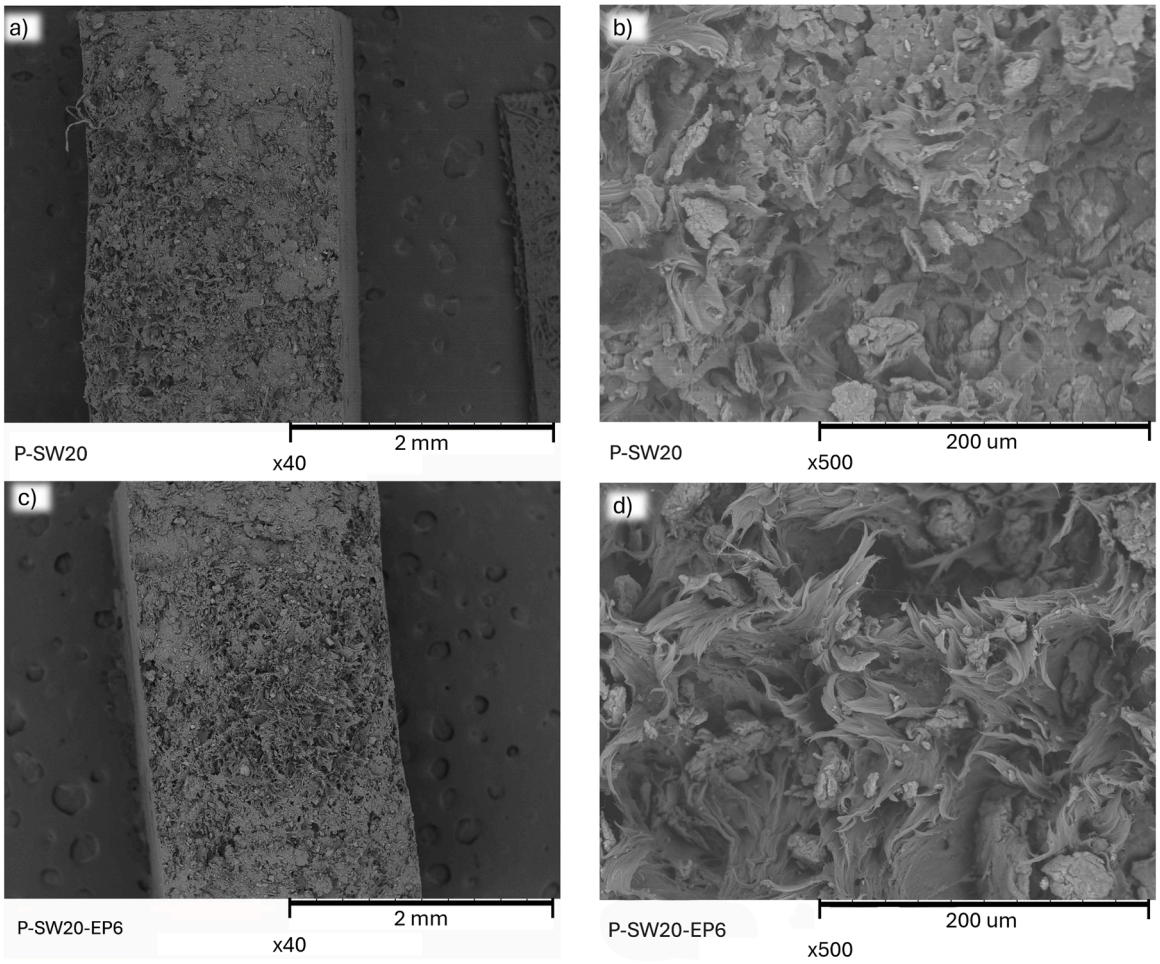

Fig. 7. SEM analysis. a) P-SW20, magnification x40. b) P-SW20, magnification x500. c) P-SW20-EP6, magnification x40. d) P-SW20-EP6, magnification x500.

Table 4
Values of L*, a* and b*, BI, chroma of P and all biocomposites prepared.

Sample name	L*	a*	b*	BI	Colour
P	80.49 ± 0.53	0.05 ± 0.22	5.19 ± 1.90	6.55	
P-SW10	24.21 ± 0.28	2.23 ± 0.07	6.47 ± 0.03	37.35	
P-SW10-EP2	30.39 ± 0.36	1.60 ± 0.03	5.22 ± 0.10	22.33	
P-SW10-EP4	30.25 ± 1.09	2.09 ± 0.20	6.04 ± 0.24	26.91	
P-SW10-EP6	32.87 ± 1.49	2.63 ± 0.17	8.18 ± 0.06	33.99	
P-SW20	24.46 ± 0.35	1.54 ± 0.29	3.40 ± 0.18	18.98	
P-SW20-EP2	23.51 ± 0.65	1.05 ± 0.09	3.41 ± 0.18	18.61	
P-SW20-EP4	22.06 ± 2.99	0.82 ± 0.18	3.41 ± 0.18	18.78	
P-SW20-EP6	26.61 ± 1.31	2.58 ± 0.05	5.3 ± 0.10	28.93	
P-SW30	20.63 ± 1.40	0.63 ± 0.05	1.98 ± 0.14	12.10	
P-SW30-EP2	26.76 ± 0.96	1.21 ± 0.09	4.10 ± 0.31	19.62	
P-SW30-EP4	27.14 ± 2.16	0.90 ± 0.06	3.22 ± 0.19	14.78	
P-SW30-EP6	27.85 ± 0.57	1.15 ± 0.02	4.60 ± 0.28	20.68	

L*: lightness; a*: redness; b*: yellowness; BI: browning index.

CRediT authorship contribution statement

Nicole Canzian: Writing – review & editing, Writing – original draft, Methodology, Formal analysis, Data curation, Conceptualization. **Valentina Beghetto:** Writing – review & editing, Writing – original draft, Methodology, Funding acquisition, Formal analysis, Data curation, Conceptualization. **Gioele Foltran:** Writing – review & editing, Formal analysis, Data curation.

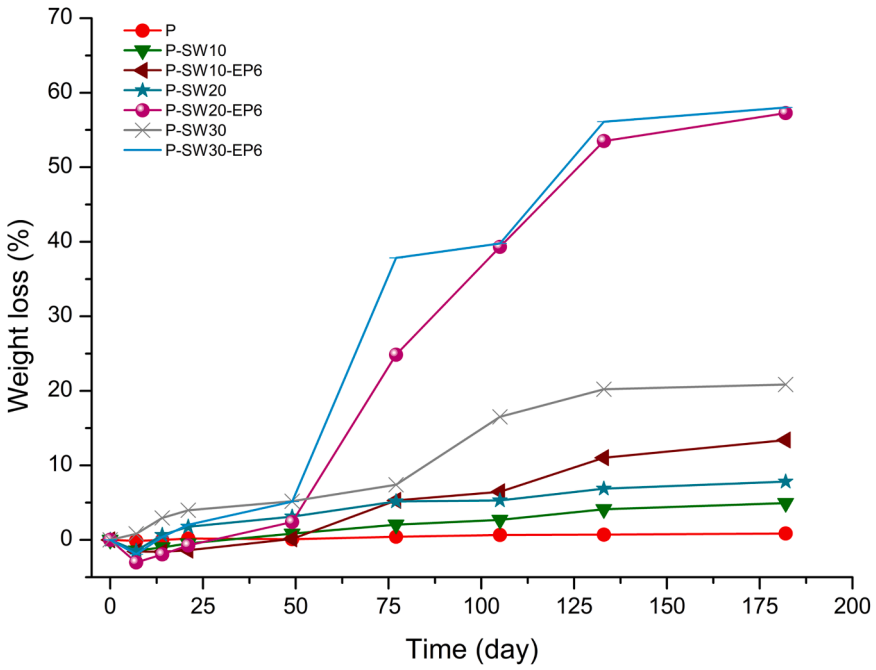

Fig. 8. Weight loss % in 183 days of the biocomposite in soil.

Declaration of Competing Interest

The authors declare that they have no known competing financial interests or personal relationships that could have appeared to influence the work reported in this paper.

Acknowledgements

The work was supported by PNRR funding for the 40th PhD cycle "Dottorato d'interesse nazionale in Desing per il Made in Italy: Identità, Innovazione e Sostenibilità", administrative headquarter University Vanvitelli, Caserta (Italy). "Food-4-Life - Alimenti funzionali per la salute e benessere: Innovazione delle materie prime, caratterizzazione delle proteine di origine vegetale e animale, nuovi approcci per la shelf life e packaging più sostenibile" - CUP: D19J24000670007 - funding PR Veneto FESR 2021–2027. The authors wish to thank Prof. Francesco Valentino and Dr. Chiara Facca for their help.

Appendix A. Supporting information

Supplementary data associated with this article can be found in the online version at doi:10.1016/j.mtcomm.2026.115228.

Data availability

Data will be made available on request.

References

[1] Plastics – the fast Facts 2024 • Plastics Europe, Plast. Eur. (n.d.). ⟨https://plasticseurope.org/knowledge-hub/plastics-the-fast-facts-2024/⟩ (accessed February 24, 2026).
[2] M. Barletta, C. Aversa, M. Ayyoob, A. Gisario, K. Hamad, M. Mehrpouya, H. Vahabi, Poly(butylene succinate) (PBS): materials, processing, and industrial applications, Prog. Polym. Sci. 132 (2022) 101579, https://doi.org/10.1016/j.progpolymsci.2022.101579.
[3] S. Huang, Q. Dong, S. Che, R. Li, K.H.D. Tang, Bioplastics and biodegradable plastics: a review of recent advances, feasibility and cleaner production, Sci. Total Environ. 969 (2025) 178911, https://doi.org/10.1016/j.scitotenv.2025.178911.
[4] A. Jayakumar, S. Radoor, S. Siengchin, G.H. Shin, J.T. Kim, Recent progress of bioplastics in their properties, standards, certifications and regulations: a review, Sci. Total Environ. 878 (2023) 163156, https://doi.org/10.1016/j.scitotenv.2023.163156.
[5] G. Bishop, D. Styles, P.N.L. Lens, Environmental performance comparison of bioplastics and petrochemical plastics: a review of life cycle assessment (LCA) methodological decisions, Resour. Conserv. Recycl 168 (2021) 105451, https://doi.org/10.1016/j.resconrec.2021.105451.
[6] S.S. Ali, E.A. Abdelkarim, T. Elsamahy, R. Al-Tohamy, F. Li, M. Kornaros, A. Zuorro, D. Zhu, J. Sun, Bioplastic production in terms of life cycle assessment: a state-of-the-art review, Environ. Sci. Ecotechnol. 15 (2023) 100254, https://doi.org/10.1016/j.ese.2023.100254.
[7] G. Atiwesh, A. Mikhael, C.C. Parrish, J. Banoub, T.-A.T. Le, Environmental impact of bioplastic use: a review, Heliyon 7 (2021) e07918, https://doi.org/10.1016/j.heliyon.2021.e07918.
[8] L. Senila, E. Kovacs, M.-A. Resz, M. Senila, A. Becze, C. Roman, Life Cycle Assessment (LCA) of Bioplastics Production from Lignocellulosic Waste (Study Case: PLA and PHB), Polymers 16 (2024) 3330, https://doi.org/10.3390/polym16233330.
[9] European Commission. Joint Research Centre., Target EU 2030, (n.d.). ⟨https://commission.europa.eu/energy-climate-change-environment/overall-targets-and-reporting/2030-targets_en⟩ (accessed February 24, 2026).
[10] V. Beghetto, V. Gatto, R. Samiolo, C. Scolaro, S. Brahimi, M. Facchin, A. Visco, Plastics today: Key challenges and EU strategies towards carbon neutrality: a review, Environ. Pollut. 334 (2023) 122102, https://doi.org/10.1016/j.envpol.2023.122102.
[11] V. Beghetto, R. Sole, C. Buranello, M. Al-Abkal, M. Facchin, Recent advancements in plastic packaging recycling: a mini-review, Materials 14 (2021) 4782, https://doi.org/10.3390/ma14174782.
[12] Agenda 2030, (n.d.). ⟨https://unric.org/it/agenda-2030/⟩ (accessed February 24, 2026).
[13] A. Sharma, S. Kulshreshtha, N.S. Rajput, A. Goyal, Utilization of jute waste in polybutylene succinate-based biocomposites and analysis of mechanical properties and biodegradability, Nat. Environ. Pollut. Technol. 24 (2025) B4267, https://doi.org/10.46488/NEPT.2025.v24i03.B4267.
[14] H. Ahmad, G. Chhipi-Shrestha, K. Hewage, R. Sadiq, A comprehensive review on construction applications and life cycle sustainability of natural fiber biocomposites, Sustainability 14 (2022) 15905, https://doi.org/10.3390/su142315905.
[15] R. Banu J, G. Sharmila V, Review on food waste valorisation for bioplastic production towards a circular economy: sustainable approaches and biodegradability assessment, Sustain. Energy Fuels 7 (2023) 3165–3184, https://doi.org/10.1039/D3SE00500C.
[16] R. Kumar, V. Lalnundiki, S.D. Shelare, G.J. Abhishek, S. Sharma, D. Sharma, A. Kumar, M. Abbas, An investigation of the environmental implications of bioplastics: recent advancements on the development of environmentally friendly bioplastics solutions, Environ. Res. 244 (2024) 117707, https://doi.org/10.1016/j.envres.2023.117707.
[17] M.M. Abe, J.R. Martins, P.B. Sanvezzo, J.V. Macedo, M.C. Branciforti, P. Halley, V.R. Botaro, M. Brienzo, Advantages and disadvantages of bioplastics production from starch and lignocellulosic components, Polymers 13 (2021) 2484, https://doi.org/10.3390/polym13152484.

[18] V. Beghetto, S. Conca, D. Santandrea, Carboxymethyl cellulose-based films for sustainable food packaging: modification strategies and structure–property relationships, Polymers 18 (2026) 552, https://doi.org/10.3390/polym18050552.
[19] A. Raschka, M. Carus, S. Piotrowski, Renewable Raw Materials and Feedstock for Bioplastics, in: S. Kabasci (Ed.), Bio-Based Plast, 1st ed., Wiley, 2013, pp. 331–345, https://doi.org/10.1002/9781118676646.ch13.
[20] X. Zhao, Y. Wang, X. Chen, X. Yu, W. Li, S. Zhang, X. Meng, Z.-M. Zhao, T. Dong, A. Anderson, A. Aiyedun, Y. Li, E. Webb, Z. Wu, V. Kunc, A. Ragauskas, S. Ozcan, H. Zhu, Sustainable bioplastics derived from renewable natural resources for food packaging, Matter 6 (2023) 97–127, https://doi.org/10.1016/j.matt.2022.11.006.
[21] H.R. Ghatak, Biorefineries from the perspective of sustainability: feedstocks, products, and processes, Renew. Sustain. Energy Rev. 15 (2011) 4042–4052, https://doi.org/10.1016/j.rser.2011.07.034.
[22] J. Brizga, K. Hubacek, K. Feng, The Unintended Side Effects of Bioplastics: Carbon, Land, and Water Footprints, One Earth 3 (2020) 45–53, https://doi.org/10.1016/j.oneear.2020.06.016.
[23] V. Beghetto, V. Gatto, S. Conca, Could fostering alternative plant feedstocks improve the sustainability of leather manufacturing? A critical review, Materials 18 (2025) 3759, https://doi.org/10.3390/ma18163759.
[24] A. Visco, C. Scolaro, M. Facchin, S. Brahimi, H. Belhamdi, V. Gatto, V. Beghetto, Agri-food wastes for bioplastics: European prospective on possible applications in their second life for a circular economy, Polymers 14 (2022) 2752, https://doi.org/10.3390/polym14132752.
[25] V. Beghetto, Waste cooking oils into high-value products: where is the industry going? Polymers 17 (2025) 887, https://doi.org/10.3390/polym17070887.
[26] X. Kang, Z. Xia, R. Chen, P. Liu, W. Yang, Effects of inorganic cations and organic polymers on the physicochemical properties and microfabrics of kaolinite suspensions, Appl. Clay Sci. 176 (2019) 38–48, https://doi.org/10.1016/j.clay.2019.04.024.
[27] Z. Ali, M. Abdullah, M.T. Yasin, K. Amanat, K. Ahmad, I. Ahmed, M.M. Qaisrani, J. Khan, Organic waste-to-bioplastics: conversion with eco-friendly technologies and approaches for sustainable environment, Environ. Res. 244 (2024) 117949, https://doi.org/10.1016/j.envres.2023.117949.
[28] V.K. Gaur, P. Gaur, A. Telegin, R.S. Thakur, P. Sharma, P. Gupta, K. Dhakar, Y. Raheja, J.K. Srivastava, S. Varjani, J.W.C. Wong, H.Y. Ng, M. Vithanage, Unlocking the potential of food waste chemistry for biodegradable plastics production: recent advancements, perspectives, and life-cycle assessment, Trends Food Sci. Technol. 156 (2025) 104836, https://doi.org/10.1016/j.tifs.2024.104836.
[29] A. Hejna, M. Barczewski, P. Kosmela, J. Aniśko, J. Szulc, K. Skórczewska, A. Piasecki, T. Kuang, More than just a beer – Brewers' spent grain, spent hops, and spent yeast as potential functional fillers for polymer composites, Waste Manag 180 (2024) 23–35, https://doi.org/10.1016/j.wasman.2024.03.023.
[30] A. Hejna, J. Korol, P. Kosmela, A. Kuzmin, A. Piasecki, A. Kulawik, B. Chmielnicki, By-products from Food Industry as a promising alternative for the conventional fillers for wood–polymer composites, Polymers 13 (2021) 893, https://doi.org/10.3390/polym13060893.
[31] V. Beghetto, Strategies for the transformation of waste cooking oils into high-value products: a critical review, Polymers 17 (2025) 368, https://doi.org/10.3390/polym17030368.
[32] T.A. Swetha, A. Bora, K. Mohanrasu, P. Balaji, R. Raja, K. Ponnuchamy, G. Muthusamy, A. Arun, A comprehensive review on polylactic acid (PLA) – synthesis, processing and application in food packaging, Int. J. Biol. Macromol. 234 (2023) 123715, https://doi.org/10.1016/j.ijbiomac.2023.123715.
[33] A. Pokharel, K.J. Falua, A. Babaei-Ghazvini, B. Acharya, Biobased polymer composites: a review, J. Compos. Sci. 6 (2022) 255, https://doi.org/10.3390/jcs6090255.
[34] L. Liu, J. Yu, L. Cheng, W. Qu, Mechanical properties of poly(butylene succinate) (PBS) biocomposites reinforced with surface modified jute fibre, Compos. Part Appl. Sci. Manuf. 40 (2009) 669–674, https://doi.org/10.1016/j.compositesa.2009.03.002.
[35] T. Cionita, M.H.M. Hamdan, J.P. Siregar, D.F. Fitriyana, R. Junid, W.L. Shing, J. Jaafar, A.P. Irawan, T. Rihayat, R. Ismail, A.P. Bayuseno, E. Jehadus, Overview of jute fibre as thermoplastic matrix polymer reinforcement, J. Renew. Mater. 12 (2024) 457–483, https://doi.org/10.32604/jrm.2024.045814.
[36] H.A. Saffian, M. Yamaguchi, H. Ariffin, K. Abdan, N.K. Kassim, S.H. Lee, C.H. Lee, A.R. Shafi, A. Humairah Alias, Thermal, physical and mechanical properties of poly(butylene succinate)/kenaf core fibers composites reinforced with esterified lignin, Polymers 13 (2021) 2359, https://doi.org/10.3390/polym13142359.
[37] A. Hejna, M. Barczewski, P. Kosmela, O. Mysiukiewicz, J. Aniśko, P. Sulima, J. Andrzej Przyborowski, M. Reza Saeb, The impact of thermomechanical and chemical treatment of waste Brewers' spent grain and soil biodegradation of sustainable Mater-Bi-Based biocomposites, Waste Manag 154 (2022) 260–271, https://doi.org/10.1016/j.wasman.2022.10.007.
[38] J. Bellon, F. Bacoup, S. Marais, R. Gattin, PLA, PBS, and PBAT Biocomposites—Part A: Matrix–Filler Interactions with Agro-Industrial Waste Fillers (Brewer's Spent Grain, Orange Peel) and Their Influence on Thermal, Mechanical, and Water Sorption Properties, Materials 18 (2025) 3867, https://doi.org/10.3390/ma18163867.
[39] A. Visco, N. Bardella, C. Scolaro, H. Belhamdi, S. Brahimi, V. Gatto, R. Samiolo, V. Beghetto, Reuse of beer spent grain for the industrial production of biodegradable bio-composites, Ind. Crops Prod. 235 (2025) 121684, https://doi.org/10.1016/j.indcrop.2025.121684.
[40] A. Gowman, T. Wang, A. Rodriguez-Uribe, A.K. Mohanty, M. Misra, Bio-poly (butylene succinate) and its composites with grape pomace: mechanical performance and thermal properties, ACS Omega 3 (2018) 15205–15216, https://doi.org/10.1021/acsomega.8b01675.
[41] T. Tschichold, G. Mäder, S. Yildirim, Characterization of PBS and PBAT biocomposites reinforced with rapeseed press cake: Influence of filler content and particle size, Mater. Today Commun. 47 (2025) 113214, https://doi.org/10.1016/j.mtcomm.2025.113214.
[42] A. Ibáñez-García, A. Martínez-García, S. Ferrándiz-Bou, Influence of almond shell content and particle size on mechanical properties of starch-based biocomposites, Waste Biomass-.-. Valoriz. 12 (2021) 5823–5836, https://doi.org/10.1007/s12649-020-01330-9.
[43] U. Akbar, A. Altaf, S.A. Mondol, U.S. Sidiqi, A.H. Dar, K.K. Dash, I. Bashir, Almond shell utilization in next-generation biocomposite packaging: a review, Trends Food Sci. Technol. 164 (2025) 105258, https://doi.org/10.1016/j.tifs.2025.105258.
[44] R.D. Bairwan, A. Khalil H.P.S, A. Nuryawan, M.I. Ahmad, M.H.M. Kassim, A. Ahmad, Enhancing biopolymer materials with coffee waste-derived reinforcements, Polym. Eng. Sci. 65 (2025) 455–477, https://doi.org/10.1002/pen.27046.
[45] G. Mäder, N. Rüegg, T. Tschichold, S. Yildirim, Utilizing spent coffee grounds as sustainable fillers in biopolymer composites: influence of particle size and content, Sustain. Food Technol. 3 (2025) 1151–1163, https://doi.org/10.1039/D5FB00187K.
[46] Y. Fang, Z. Jiang, X. Zhao, J. Dong, X. Li, Q. Zhang, Spent coffee Grounds/Poly (butylene succinate) biocomposites with Robust mechanical property and heat resistance via reactive compatibilization, Compos. Commun. 29 (2022) 101003, https://doi.org/10.1016/j.coco.2021.101003.
[47] M. Ortenzi, H. Farina, S. Yildirim, S. Gazzotti, C. Strigini, S. Miescher, Potato Peels as Biobased Fillers for Poly Butylene Succinate Composites: The Role of Pla-Based Compatibilizing Agents Towards New-Generation Food Packaging Materials, (2025). https://doi.org/10.2139/ssrn.5243355.
[48] E. Sasimowski, M. Majewski, Grochowicz, Study on the biodegradation of poly (butylene succinate)/wheat bran biocomposites, Materials 16 (2023) 6843, https://doi.org/10.3390/ma16216843.
[49] G. Strangis, D. Rossi, P. Cinelli, M. Seggiani, Seawater biodegradable poly (butylene succinate-co-adipate)—wheat bran biocomposites, Materials 16 (2023) 2593, https://doi.org/10.3390/ma16072593.
[50] S. Sushri, K. Elavarasan, M. Safeena, H. Devi, C. Tejpal, Valorisation of seaweed waste from agar processing industry, Examines Mar. Biol. Oceano 5 (2023), https://doi.org/10.31031/EIMBO.2023.05.000614.
[51] N.A. Chudasama, R.A. Sequeira, K. Moradiya, K. Prasad, Seaweed polysaccharide based products and materials: an assessment on their production from a sustainability point of view, Molecules 26 (2021) 2608, https://doi.org/10.3390/molecules26092608.
[52] K. Mondal, P. Bhagabati, V.V. Goud, S. Sakurai, V. Katiyar, Utilization of microalgae residue and isolated cellulose nanocrystals: A study on crystallization kinetics of poly(ε-caprolactone) bio-composites, Int. J. Biol. Macromol. 191 (2021) 521–530, https://doi.org/10.1016/j.ijbiomac.2021.09.114.
[53] E. Lizundia, F. Luzi, D. Puglia, Organic waste valorisation towards circular and sustainable biocomposites, Green. Chem. 24 (2022) 5429–5459, https://doi.org/10.1039/D2GC01668K.
[54] K.M. Zia, M. Zuber, M. Ali. Algae Based Polymers, Blends, and Composites: Chemistry, Biotechnology and Materials Science, Elsevier, 2017.
[55] H.S. El-Beltagi, A.A. Mohamed, H.I. Mohamed, K.M.A. Ramadan, A.A. Barqawi, A.T. Mansour, Phytochemical and potential properties of seaweeds and their recent applications: a review, Mar. Drugs 20 (2022) 342, https://doi.org/10.3390/md20060342.
[56] C.M. Duarte, N. Marbá, M. Holmer, Rapid domestication of marine species, Science 316 (2007) 382–383, https://doi.org/10.1126/science.1138042.
[57] A. Annam Renita, P. Senthil Kumar, Valorization of Waste Algal Boom for Value-Added Products, in: M. Jerold, S. Arockiasamy, V. Sivasubramanian (Eds.), Bioprocess Eng. Bioremediation, Springer International Publishing, Cham, 2020, pp. 129–137, https://doi.org/10.1007/698_2020_579.
[58] D. Burhani, A.Wijayanto Sudarmanto, I. Andreansyah, Y. Widyawati, Y. Nurhamiyah, D. Fransiska, S. Agustina, W.Banar Kusumaningrum, W. Fatriasari, F.Aulya Syamani, Utilization of Indonesian seaweed in polyethylene-based composite with coconut husk powder as bio-compatibilizer, Mater. Today Proc. (2023) S2214785323018370, https://doi.org/10.1016/j.matpr.2023.03.765.
[59] S. Iannace, G. Nocilla, L. Nicolais, Biocomposites based on sea algae fibers and biodegradable thermoplastic matrices, J. Appl. Polym. Sci. 73 (1999) 583–592, https://doi.org/10.1002/(SICI)1097-4628(19990725)73:4%253C583::AID-APP14%253E3.0.CO;2-H.
[60] E. Chiellini, P. Cinelli, V.I. Ilieva, M. Martera, Biodegradable Thermoplastic Composites Based on Polyvinyl Alcohol and Algae, Biomacromolecules 9 (2008) 1007–1013, https://doi.org/10.1021/bm701041e.
[61] R. Karthikeyan, S. Madhu, Impact of brown algae particles on the mechanical properties of jute-reinforced polymeric composites for sustainable development, Results Eng. 25 (2025) 104548, https://doi.org/10.1016/j.rineng.2025.104548.
[62] G.M. Kim, W.-S. Chang, Y.-K. Kim, Biocomposites Using Whole or Valuable Component-Extracted Microalgae Blended with Polymers: A Review, Catalysts 12 (2021) 25, https://doi.org/10.3390/catal12010025.
[63] A. Barghini, V.I. Ivanova, S.H. Imam, E. Chiellini, Poly-(ε-caprolactone) (PCL) and poly(hydroxy-butyrate) (PHB) blends containing seaweed fibers: Morphology and

thermal-mechanical properties, J. Polym. Sci. Part Polym. Chem. 48 (2010) 5282–5288, https://doi.org/10.1002/pola.24327.
[64] M.W. Lee, S.O. Han, Y.B. Seo, Red algae fibre/poly(butylene succinate) biocomposites: The effect of fibre content on their mechanical and thermal properties, Compos. Sci. Technol. 68 (2008) 1266–1272, https://doi.org/10.1016/j.compscitech.2007.12.016.
[65] K.J. Sim, S.O. Han, Y.B. Seo, Dynamic mechanical and thermal properties of red algae fiber reinforced poly(lactic acid) biocomposites, Macromol. Res. 18 (2010) 489–495, https://doi.org/10.1007/s13233-010-0503-3.
[66] C. Toro, M.M. Reddy, R. Navia, M. Rivas, M. Misra, A.K. Mohanty, Characterization and application in biocomposites of residual microalgal biomass generated in third generation biodiesel, J. Polym. Environ. 21 (2013) 944–951, https://doi.org/10.1007/s10924-013-0609-8.
[67] B. Ferrero, V. Fombuena, O. Fenollar, T. Boronat, R. Balart, Development of natural fiber-reinforced plastics (NFRP) based on biobased polyethylene and waste fibers from *Posidonia oceanica* seaweed, Polym. Compos 36 (2015) 1378–1385, https://doi.org/10.1002/pc.23042.
[68] T.J. Madera-Santana, Y. Freile-Pelegrín, J.C. Encinas, C.R. Ríos-Soberanis, P. Quintana-Owen, Biocomposites based on poly(lactic acid) and seaweed wastes from agar extraction: Evaluation of physicochemical properties, J. Appl. Polym. Sci. 132 (2015) app.42320, https://doi.org/10.1002/app.42320.
[69] N. Zhu, M. Ye, D. Shi, M. Chen, Reactive compatibilization of biodegradable poly (butylene succinate)/Spirulina microalgae composites, Macromol. Res. 25 (2017) 165–171, https://doi.org/10.1007/s13233-017-5025-9.
[70] T. Garrido, M. Peñalba, K. De La Caba, P. Guerrero, Injection-manufactured biocomposites from extruded soy protein with algae waste as a filler, Compos. Part B Eng. 86 (2016) 197–202, https://doi.org/10.1016/j.compositesb.2015.09.058.
[71] Farah Nurasyikin Md Rosdi, Nurjannah Salim, Rasidi Roslan, Nurul Huda Abu Bakar, Siti Noorbaini Sarmin, Potential Red Algae Fibre Waste as a Raw Material for Biocomposite, Adv. Res. Appl. Sci. Eng. Technol. 30 (2023) 303–310, https://doi.org/10.37934/araset.30.1.303310.
[72] B. Ahmed, A Critical Review on PLA-Algae Composite, Chem. Mech. Therm. Prop. 10 (2020).
[73] M. Bulota, T. Budtova, Valorisation of macroalgae industrial by-product as filler in thermoplastic polymer composites, Compos. Part Appl. Sci. Manuf. 90 (2016) 271–277, https://doi.org/10.1016/j.compositesa.2016.07.010.
[74] M. Bulota, T. Budtova, PLA/algae composites: Morphology and mechanical properties, Compos. Part Appl. Sci. Manuf. 73 (2015) 109–115, https://doi.org/10.1016/j.compositesa.2015.03.001.
[75] C. Ververis, K. Georghiou, D. Danielidis, D.G. Hatzinikolaou, P. Santas, R. Santas, V. Corleti, Cellulose, hemicelluloses, lignin and ash content of some organic materials and their suitability for use as paper pulp supplements, Bioresour. Technol. 98 (2007) 296–301, https://doi.org/10.1016/j.biortech.2006.01.007.
[76] H. Jeong, J. Park, H. Kim, Determination of NH4+ in Environmental Water with Interfering Substances Using the Modified Nessler Method, J. Chem. 2013 (2013) 359217, https://doi.org/10.1155/2013/359217.
[77] IRSA-CNR, Analytical methods for water, (2003).
[78] R. Pangestuti, M. Haq, P. Rahmadi, B.-S. Chun, Nutritional Value and Biofunctionalities of Two Edible Green Seaweeds (Ulva lactuca and Caulerpa racemosa) from Indonesia by Subcritical Water Hydrolysis, Mar. Drugs 19 (2021) 578, https://doi.org/10.3390/md19100578.
[79] Z. Huang, L. Qian, Q. Yin, N. Yu, T. Liu, D. Tian, Biodegradability studies of poly (butylene succinate) composites filled with sugarcane rind fiber, Polym. Test. 66 (2018) 319–326, https://doi.org/10.1016/j.polymertesting.2018.02.003.
[80] ASTM D638, Standard for Plastic Tensile Testing, (n.d.).
[81] ASTM D618, Standard Practice for Conditioning Plastics for Testing, (n.d.).
[82] UNI EN 13038, Soil improvers and growing media - Determination of electrical conductivity, (2012).
[83] UNI EN 13037, Soil improvers and growing media - Determination of pH., (2012).
[84] UNI EN 13041, Soil improvers and growing media - Determination of physical properties - Dry bulk density, air volume, Water Vol. shrinkage Coeff. Total porosity (2012).
[85] C. Medina Jaramillo, T.J. Gutiérrez, S. Goyanes, C. Bernal, L. Famá, Biodegradability and plasticizing effect of yerba mate extract on cassava starch edible films, Carbohydr. Polym. 151 (2016) 150–159, https://doi.org/10.1016/j.carbpol.2016.05.025.
[86] D. Santandrea, C. Sillard, V. Beghetto, J. Bras, Aqueous-Phase Surface Amidation of TEMPO-CNF Films for Improved Adsorption of Organic Pollutants in Water, ChemPlusChem 90 (2025) e202500398, https://doi.org/10.1002/cplu.202500398.
[87] G. Gamero-Vega, M. Palacios-Palacios, V. Quitral, Nutritional composition and bioactive compounds of red seaweed: a mini-review, Sci. Educ. Publ. 8 (2020) 431–440, https://doi.org/10.12691/jfnr-8-8-7.
[88] S. Wang, Q. Xing, Study on properties and biocompatibility of poly (butylene succinate) and sodium alginate biodegradable composites for biomedical applications, Mater. Res. Express 9 (2022) 085403, https://doi.org/10.1088/2053-1591/ac896f.
[89] R. Turco, S. Mallardo, D. Zannini, A. Moeini, M.D. Serio, R. Tesser, P. Cerruti, G. Santagata, Dual role of epoxidized soybean oil (ESO) as plasticizer and chain extender for biodegradable polybutylene succinate (PBS) formulations, Giant 20 (2024) 100328, https://doi.org/10.1016/j.giant.2024.100328.
[90] X. Wang, J. Zhou, L. Li, Multiple melting behavior of poly(butylene succinate), Eur. Polym. J. 43 (2007) 3163–3170, https://doi.org/10.1016/j.eurpolymj.2007.05.013.
[91] S. Pivsa-Art, W. Pivsa-Art, Eco-friendly bamboo fiber-reinforced poly(butylene succinate) biocomposites, Polym. Compos 42 (2021) 1752–1759, https://doi.org/10.1002/pc.25930.
[92] Z. Qi, H. Ye, J. Xu, J. Chen, B. Guo, Improved the thermal and mechanical properties of poly(butylene succinate-co-butylene adipate) by forming nanocomposites with attapulgite, Colloids Surf. Physicochem. Eng. Asp. 421 (2013) 109–117, https://doi.org/10.1016/j.colsurfa.2012.12.051.
[93] N. Khan, K. Sudhakar, R. Mamat, Thermogravimetric Analysis of Marine Macroalgae Waste Biomass as Bio-Renewable Fuel, J. Chem. 2022 (2022) 1–9, https://doi.org/10.1155/2022/6417326.
[94] A.K. Zykova, P.V. Pantyukhov, N.N. Kolesnikova, T.V. Monakhova, A.A. Popov, Influence of filler particle size on physical properties and biodegradation of biocomposites based on low-density polyethylene and lignocellulosic fillers, J. Polym. Environ. 26 (2018) 1343–1354, https://doi.org/10.1007/s10924-017-1039-9.
[95] A. Hejna, Poly(ε-Caprolactone)/Brewers' Spent Grain Composites—The Impact of Filler Treatment on the Mechanical Performance, J. Compos. Sci. 4 (2020) 167, https://doi.org/10.3390/jcs4040167.
[96] H. Salmah, A. Romisuhani, H. Akmal, Properties of low-density polyethylene/palm kernel shell composites: Effect of polyethylene co-acrylic acid, J. Thermoplast. Compos. Mater. 26 (2013) 3–15, https://doi.org/10.1177/0892705711417028.
[97] Z.N. Terzopoulou, G.Z. Papageorgiou, E. Papadopoulou, E. Athanassiadou, M. Reinders, D.N. Bikiaris, Development and study of fully biodegradable composite materials based on poly(butylene succinate) and hemp fibers or hemp shives, Polym. Compos. 37 (2016) 407–421, https://doi.org/10.1002/pc.23194.
[98] P. Liminana, D. Garcia-Sanoguera, L. Quiles-Carrillo, R. Balart, N. Montanes, Development and characterization of environmentally friendly composites from poly(butylene succinate) (PBS) and almond shell flour with different compatibilizers, Compos. Part B Eng. 144 (2018) 153–162, https://doi.org/10.1016/j.compositesb.2018.02.031.
[99] A. Barth, Infrared spectroscopy of proteins, Biochim. Biophys. Acta BBA - Bioenerg. 1767 (2007) 1073–1101, https://doi.org/10.1016/j.bbabio.2007.06.004.
[100] I. Ahmed, M.B.K. Niazi, A. Hussain, Z. Jahan, Influence of amphiphilic plasticizer on properties of thermoplastic starch films, Polym. -Plast. Technol. Eng. 57 (2018) 17–27, https://doi.org/10.1080/03602559.2017.1298803.
[101] B. Yousif, S. Tayeb, Mechanical and wear properties of oil palm and glass fibres reinforced polyester composites, Int. J. Precis. Technol. 1 (2009), https://doi.org/10.1504/IJPTECH.2009.026380.
[102] D. Santandrea, V. Beghetto, 4-(4,6-Dimethoxy-1,3,5-triazin-2-yl)-4-methyl-morpholinium chloride-assisted amide crosslinking of carboxymethyl cellulose for high-performing films, RSC Adv. 15 (2025) 34846–34860, https://doi.org/10.1039/D5RA05273D.
[103] V. Beghetto, V. Gatto, S. Conca, N. Bardella, C. Buranello, G. Gasparetto, R. Sole, Development of 4-(4,6-dimethoxy-1,3,5-triazin-2-yl)-4-methyl-morpholinium chloride cross-linked carboxymethyl cellulose films, Carbohydr. Polym. 249 (2020) 116810, https://doi.org/10.1016/j.carbpol.2020.116810.
[104] J. Joy, C. Jose, X. Yu, L. Mathew, S. Thomas, S. Pilla, The influence of nanocellulosic fiber, extracted from Helicteres isora, on thermal, wetting and viscoelastic properties of poly(butylene succinate) composites, Cellulose 24 (2017), https://doi.org/10.1007/s10570-017-1439-y.
[105] A. Fajraoui, J.B. Nasr, C. Lacoste, P. Dony, S. Odof, M.B. Amar, F.E. Halouani, Elaboration of a bio-colored material based on natural dye and polybutylene succinate: comparative study with colored polylactic acid, J. Polym. Environ. 30 (2022) 1673–1681, https://doi.org/10.1007/s10924-021-02309-w.